Numerical comparison of acoustic wedge models, with application to ultrasonic telemetry

B. Lü [a,b,c,d], M. Darmon [b,*], L. Fradkin [e], C. Potel [c,d]

[a] *M2M China, 6F, West Building, La De Fang Si, 1480 Tianfu Avenue, Chengdu, Sichuan 610041, PR China*
[b] *CEA, LIST, Department of Imaging & Simulation for Nondestructive Testing, F-91191 Gif-sur-Yvette, France*
[c] *LUNAM Université, Université du Maine, CNRS UMR 6613, Laboratoire d'Acoustique de l'Université du Maine, Le Mans, France*
[d] *Fédération Acoustique du Nord Ouest (FANO), FR CNRS 3110, France*
[e] *Sound Mathematics Ltd., Cambridge CB4 2AS, UK*

Ultrasonic telemetry imaging systems are used to monitor such immersed structures as main vessels of nuclear reactors. The interaction between acoustic beams and targets involves scattering phenomena, mainly specular reflection and tip diffraction. In order to assist in the design of imaging systems, a simulation tool is required for the accurate modeling of such phenomena. Relevant high-frequency scattering models have been developed in electromagnetic applications, in particular, the geometrical optics (GO), Geometrical Theory of Diffraction (GTD) and its uniform corrections (UAT and UTD), Kirchhoff approximation (KA) and Physical Theory of Diffraction (PTD). Before adopting any of them for simulation of scattering of acoustic waves by edged immersed rigid bodies, it is important to realize that in acoustics the characteristic dimension to the wave length ratio is usually considerably smaller than in electromagnetics and a further study is required to identify models' advantages, disadvantages and regions of applicability. In this paper their numerical comparison is carried out. As the result, the most suitable algorithm is identified for simulating ultrasonic telemetry of immersed rigid structures.

1. Introduction

An ultrasonic telemetry imaging system reported in [1] allows its operators to monitor position of structures immersed in opaque liquids, ensuring continual safe operation of such structures. One of its possible applications is in monitoring the core of a sodium-cooled fast-neutron reactor, a Generation IV nuclear plant design [2]. Deploying the system in conjunction with this design is particularly attractive, because sodium's opacity makes ultrasound a more effective monitoring agent than light. No significant impediments to its adoption are envisaged, since ultrasonic techniques are already widely used in industry for Non-Destructive Evaluation (NDE) of structural integrity of solid components [3].

Telemetry is the process of determining the distance between the surface of a probe emitting an acoustic beam and a bright spot on the target. This is achieved by measuring the time of flight of the echo backscattered from the target. Many parameters influence the received signal: the incident angle, signal frequency, target geometry and size, material properties of the medium carrying the beam (such as velocity fluctuations) [1,4], etc. Therefore a simulation tool [1,5] is required to allow designers to investigate and optimize the performance of the proposed system.

When an acoustic beam interacts with targets of different geometries (large planar structures or edged bodies), the most widely known scattering phenomena that take place are high-frequency effects of specular reflection and edge diffraction. Several high-frequency scattering approximations mainly developed in electromagnetism [6–11] can be used to model the high-frequency acoustic wave scattering by immersed rigid targets. Some of them are based on ray theories and others on integral formulations.

To start with the specular phenomena, when an acoustic beam impinges on a smooth (locally plane) surface its reflection/refraction can be described by the simplest ray theory known as Geometrical Optics (GO) [6,11] using Snell–Descartes law and energy conservation. When the surface has a complicated shape but can still be considered locally plane it is convenient to employ the so-called Kirchhoff approximation (KA) based on the Green's integral formalism and referred to in electromagnetism as Physical Optics (PO) [11–13].

* Corresponding author. Tel.: +33 169082288.
E-mail addresses: b.lu@m2m-ndt.com (B. Lü), michel.darmon@cea.fr (M. Darmon), l.fradkin@soundmathematics.com (L. Fradkin), catherine.potel@univ-lemans.fr (C. Potel).

Diffraction phenomena arise in presence of such surface irregularities as edges. Their quantitative description is provided by the Geometrical Theory of Diffraction (GTD) originally proposed by Keller [7]. This is another ray theory, with the directions of diffracted rays governed by the Snell–Descartes law of diffraction. The GTD [13] states that the amplitudes carried by these rays can be computed using the stationary phase asymptotics of the solution of the relevant canonical problem, that is, the problem that reproduces the main features of the local geometry. The most widely used canonical problems [12] are diffraction of a plane wave by a planar wedge and by a rigid half-plane (the 360° wedge).

GO and classical GTD provide good description of reflected/refracted and diffracted fields, respectively, but fail in transition zones. For example, if a GTD recipe is applied in a transition zone (known as penumbra) surrounding the shadow boundary (SB) between an irradiated and shadow regions the resulting diffraction coefficients possess non-physical singularities. One approach to remedying the situation is to develop a generalization of GTD as is done in the Uniform Geometrical Theory of Diffraction (UTD) [8]. This offers asymptotics of the diffracted field which are valid not only in irradiated and shadow regions but inside the penumbras as well. Another approach is to develop uniform asymptotics of the total field. One such solution is offered by the Uniform Asymptotic Theory (UAT) [9] and another, by the Physical Theory of Diffraction (PTD) [10].

In this paper the numerical comparison of the above physical theories is carried out in two-dimensional configurations using typical parameters encountered in ultrasonic NDE in order to identify the one best suited for the purpose at hand. Scattering by both a rigid half-plane and a rigid wedge is considered. Preliminary works done for the half plane are shown in Proceeding [14]. The present paper focuses on the wedge scattering problem providing new results obtained using validated UTD and PTD wedge models so that five different analytical approximations are compared in an acoustic case: GTD, UAT, UTD, KA and PTD. For instance, PTD is shown to surpass KA for the scattering near a wedge surface or in shadow zones.

2. Approximate solutions to the wedge scattering problem

Consider first a two-dimensional space filled with a homogeneous fluid supporting an acoustic speed c and containing a perfect rigid wedge of angle Φ irradiated by an acoustic plane wave incident at an angle θ_0 with one of the wedge faces (see Fig. 1). Introduce the Cartesian system with the origin at the wedge tip $\mathbf{x}_0 = (0,0)$ and the x_1-axis running along the irradiated face. Then any observation point $\mathbf{x} = (x_1, x_2)$ can also be described in terms of the corresponding polar coordinates (r, θ) (Fig. 1).

In ray theory, the resulting total field φ^t comprises the incident field φ^i, reflected field φ^r and field φ^d diffracted from the edge. Fig. 1 details – for the field incident on the upper wedge face – the illuminated and shadow zones of the incident and GO reflected fields, which are separated by straight light/shadow boundaries. Transition zones (also called penumbras) are areas surrounding shadow boundaries. Area I + R lies inside both incident, reflected and diffracted fields, $\varphi^t = \varphi^i + \varphi^r + \varphi^d$ for $0 < \theta < \pi - \theta_0$ and outside penumbra IP. Area I lies inside both incident and diffracted fields, $\varphi^t = \varphi^i + \varphi^d$ for $\pi - \theta_0 < \theta < \pi + \theta_0$ and outside penumbras IP and RP. Area S is the total shadow zone of GO; only diffracted rays penetrate it, $\varphi^t = \varphi^d$ for $\pi + \theta_0 < \theta < \Phi$ and outside penumbra RP. ISB (RSB) is the light/shadow boundary of the incident (reflected) field and separates the area illuminated by incident (reflected) rays from its corresponding shadow zone. Outside transition zones (designated "incident IP" and "reflected RP" in Fig. 1), the total field can be represented as the sum of the GO fields and the edge diffracted waves. Penumbra is the neighborhood of the shadow boundary where such a representation of the total field is inapplicable and the field exhibits a transient behavior.

We start with the edge diffracted field. It is best described by the classical GTD, which represents it as decreasing as the square root of both the distance to the edge and wave frequency and involves the so-called GTD edge diffraction coefficients D_{GTD} [7]. GTD can be obtained as the leading order term in the non-uniform asymptotic series, which apply in geometrical (illuminated and shadow) regions but not in the transition zones, such as penumbras. In particular, the GTD diffraction coefficients D_{GTD} are often infinite at SB of the incident field as well as SBs of the fields reflected from both wedge faces. By way of an example, Fig. 2 shows the diffraction coefficient of a wedge of angle $\Phi = 270°$ for the incidence angle $\theta_0 = 50°$. In this configuration, only the horizontal wedge face is illuminated and reflects the incident field, and the GTD singularities are located at $\theta = 180° - \theta_0 = 130°$ (the reflected SB) and $\theta = 180° + \theta_0 = 230°$ (the incident SB).

As mentioned in the Introduction, several uniform theories can extend the validity of GTD to penumbras.

It has been shown in [15] that to leading order, UAT and UTD give the identical description of the field scattered from a planar wedge illuminated by a plane wave. However these theories are uniform only in the absence of other transition zones outside penumbras. In particular, both are invalid in caustic regions. In the case studied here of plane wave scattering from a wedge with planar faces, the only caustic region is the edge of the wedge. Other caustics in the edge diffracted field can occur if the edge is curved

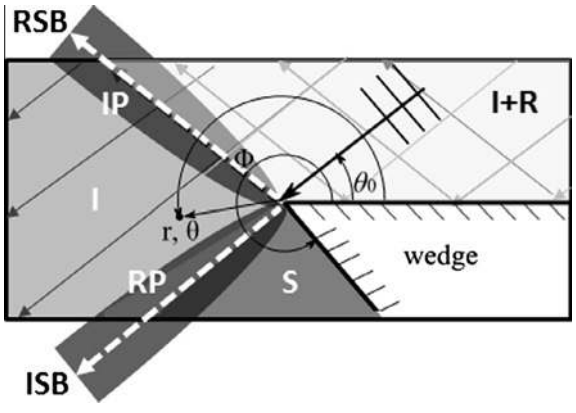

Fig. 1. Scatter of a plane wave incident at an angle θ_0 by a wedge of angle Φ. Description of illuminated and shadow areas, transition zones (penumbras) and shadow boundaries (white dashed arrows).

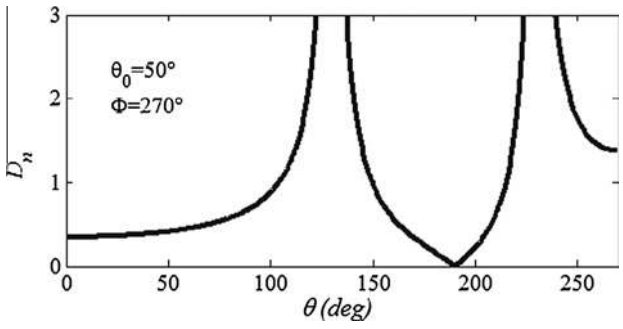

Fig. 2. GTD diffraction coefficient for $\Phi = 270°$ and $\theta_0 = 50°$. $\omega = 2\pi^*$ 1 MHz and $c = 2472$ m/s.

or the incident wave-front is concave at the diffraction point on the edge. Nevertheless, in the shadow of the reflected field, UAT relies on fictitious reflected rays [16]. Consequently, UAT fails on caustics of fictitious reflected rays: When modeling a wedge with planar faces, a caustic of this nature occurs at the image point of a point source illuminating the wedge (see Fig. 3.7 in [17]) but no such caustic arises when the incident wave is plane (see Fig. 3.6 in [17]).

Let us now turn to reflected fields. When dealing with complicated scattering surfaces it is convenient to simulate them using the Kirchhoff approximation (KA) [11,12]. KA is based on the assumption that on the wedge the scattered field can be described using the standard GO. KA provides a correct description of the specular reflection, can be applicable in a caustic vicinity and displays no singularities in penumbras. However, the KA amplitudes of diffracted waves are incorrect. This KA failure can be rectified using PTD, that is, adding an edge diffracted field with the GTD coefficient replaced by the difference $D_{\mathrm{GTD}} - D_{\mathrm{KA}}$ between GTD and KA wedge diffraction coefficients, where the latter is calculated using asymptotic evaluation of the KA solution. The difference $D_{\mathrm{GTD}} - D_{\mathrm{KA}}$ is finite everywhere, even in penumbras (see Fig. 3), so that PTD is valid uniformly in all observation directions. This approximation, initially developed in electromagnetism, has been recently extended to elastodynamics [18].

3. Numerical results

Unlike UAT and UTD, PTD cannot be used to calculate the higher order interactions. However the higher order fields are usually so much weaker than the primary fields as to be of no practical interest. Below we compare scattering models to their leading order only. Two scatterers are considered, a half-plane and a wedge of angle $\Phi = 270°$. All scattered amplitudes are normalized by the amplitude of the incident wave.

3.1. Scatter by a rigid half-plane

First we compare KA, PTD and exact solution of the problem of scatter of a plane harmonic wave by a half-plane $\{S : x_1 > 0, x_2 = 0\}$, that is, the wedge of angle $\Phi = 360°$. The exact solution has been obtained by using the Sommerfeld–Malyuzhinets technique [12]. For the half-plane, UAT reduces to the Sommerfeld's exact solution, which involves the Fresnel functions [13]. A typical discrepancy between the KA approximation and exact Sommerfeld solution can be seen in Fig. 4. The KA error is symmetric with respect to S, because the integrand in the Kirchhoff integral has two symmetrical phase stationary points (see [13]). One gives rise to the GO field reflected from the irradiated side of the half-plane and another to the fictitious field in the shadow region, which compensates the incident field there. The KA error

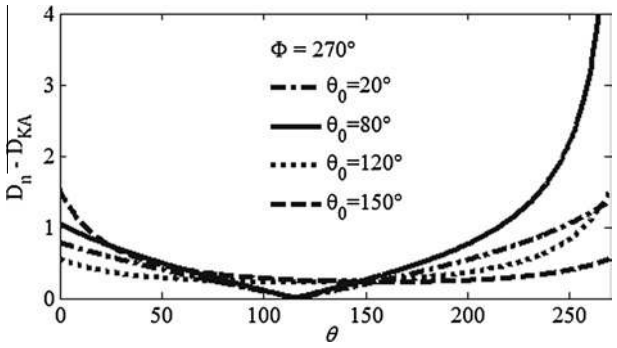

Fig. 3. Difference between the GTD and KA wedge diffraction coefficients for $\Phi = 270°$ and different incident angles θ_0. $\omega = 2\pi^*$ 1 MHz and $c = 2472$ m/s.

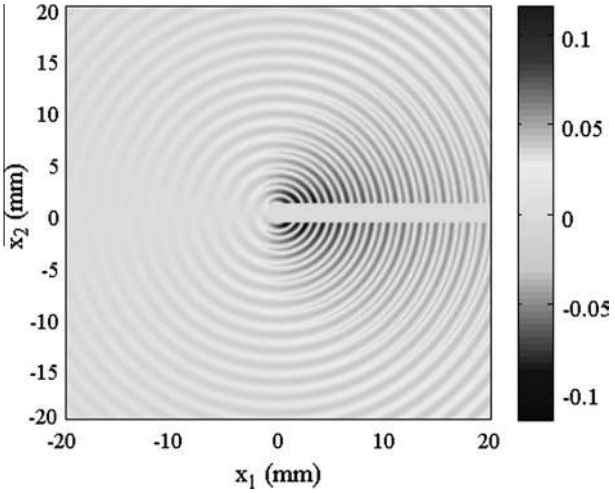

Fig. 4. The discrepancy between the normalized KA and exact amplitudes. $\Phi = 360°$, incidence angle $\theta_0 = 50°$, $\omega = 2\pi^*$ 1 MHz and $c = 2472$ m/s.

is significant only near the edge, where the GO approximation used in KA fails. A typical deviation of PTD from the exact solution is shown in Fig. 5. Comparing Figs. 4 and 5 and taking into account the difference in their amplitude scales, the largest error is reduced from 10% for KA to about 0.4% for PTD.

Fig. 6 shows the total field φ^t simulated using PTD for the same configuration as in Figs. 4 and 5. There are three geometrical areas:

- $\theta < 180° - \theta_0$ (130° – the reflected SB), where both incident and reflected fields propagate;
- $180° - \theta_0 < \theta < 180° + \theta_0$ (230° – the incident SB), where only incident field propagates;
- $\theta > 180° + \theta_0$, where there are no geometrical fields.

Unlike GO, the total PTD field exhibits a smooth variation in the vicinity of SBs and its edge cylindrical diffracted waves penetrate the common shadow zone $(\theta > 180° + \theta_0)$.

It follows that PTD combines advantages of both GTD (accurate modeling of edge diffraction) and KA (accurate modeling of geometrical field whatever the shape of smooth scatterer).

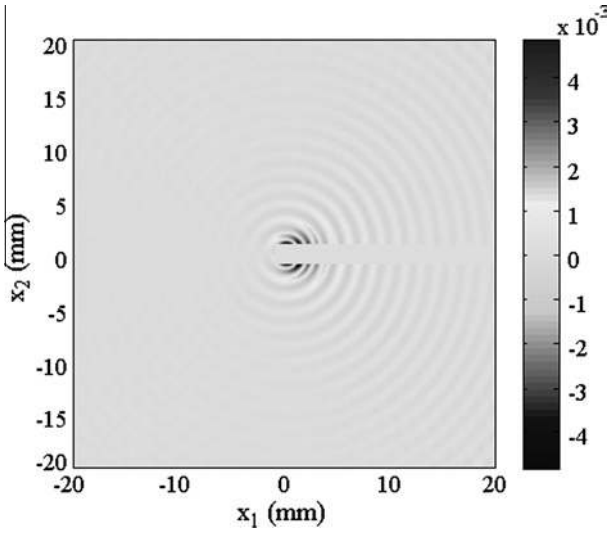

Fig. 5. The discrepancy between the normalized PTD and exact amplitudes. $\Phi = 360°$, $\theta_0 = 50°$, $\omega = 2\pi^*$ 1 MHz and $c = 2472$ m/s.

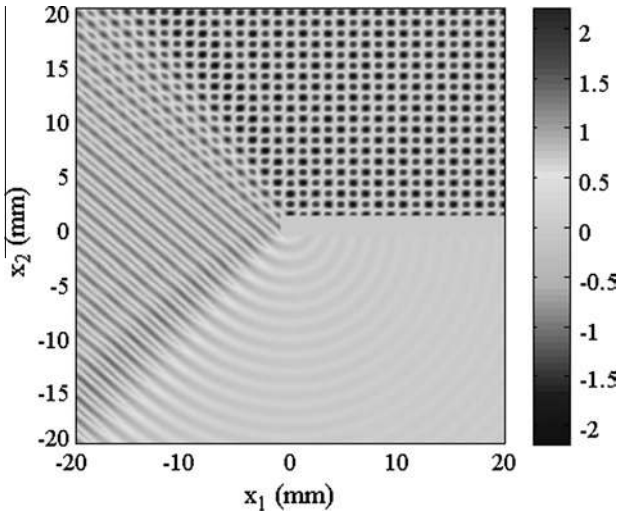

Fig. 6. The normalized total PTD field. $\Phi = 360^\circ$, $\theta_0 = 50^\circ$, $\omega = 2\pi^*$ 1 MHz and $c = 2472$ m/s.

3.2. Scatter by a rigid wedge of angle $\Phi = 270^\circ$

Let us now compare the numerical performance of the models discussed above when modeling scatter by a rigid wedge of angle $\Phi = 270^\circ$. For all wedges other than the half-plane, UAT provides not the exact solution but the best approximation to it and therefore is used as a reference in Figs. 7–10, where we plot the amplitudes of the total field normalized by the incident amplitude at the distance $r = 2\lambda$ from the wedge tip, with $\lambda = 2\pi/k$ – the wave length.

In Fig. 7 we present the total normalized GTD field simulated by adding to the edge diffracted GTD field the GO fields, both incident and reflected. The GTD singularities are observed at the shadow boundaries $\theta = 120^\circ$ and 240°. The reference UAT solution exhibits lobes for observation angles $\theta < 180^\circ - \theta_0$, where we have interference between incident, reflected and diffracted waves, and for $180^\circ - \theta_0 < \theta < 180^\circ + \theta_0$, where only interference between incident and diffracted waves takes place. As expected, outside penumbras, GTD approximation is as accurate as UAT. Fig. 8 confirms that UAT and UTD also give identical results.

Fig. 9 illustrates the KA performance, good overall, but erroneous in the shadow ($\theta > 240^\circ$). As explained above, the KA error is proportional to $D_{GTD} - D_{KA}$ and therefore there is a consistency between Figs. 3 and 9: Away from the specular direction, KA loses accuracy and requires the PTD correction to improve its modeling of edge diffracted fields. Fig. 9 also demonstrates the lack of self-consistency in KA: Near the surface the total KA field is far greater than 2 $\varphi^i(\mathbf{x}')$ (this double incident normalized amplitude is represented in Figs. 7–10 by a large circle marked 2). Finally,

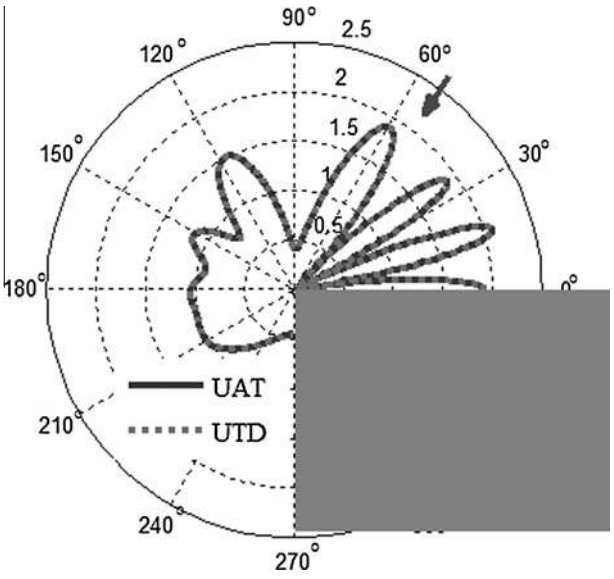

Fig. 8. Comparison between radiation patterns predicted by UAT and UTD for a rigid wedge (gray area). $\Phi = 270^\circ$, $\theta_0 = 60^\circ$ and $r = 2\lambda$; $\omega = 2\pi^*$ 1 MHz and $c = 2472$ m/s. The amplitude of the total field normalized by the incident one is plotted versus the observation angle θ in a polar diagram.

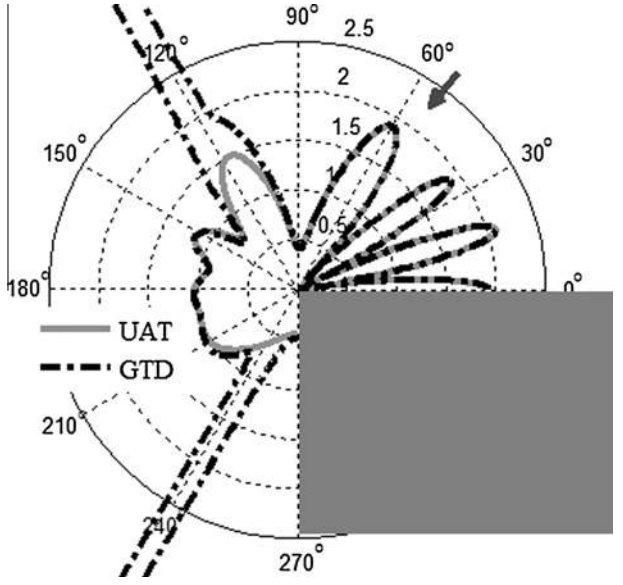

Fig. 7. Comparison between radiation patterns predicted by UAT and GTD for a rigid wedge (gray area). $\Phi = 270^\circ$, $\theta_0 = 60^\circ$ and $r = 2\lambda$; $\omega = 2\pi^*$ 1 MHz and $c = 2472$ m/s. The amplitude of the total field normalized by the incident one is plotted versus the observation angle θ in a polar diagram.

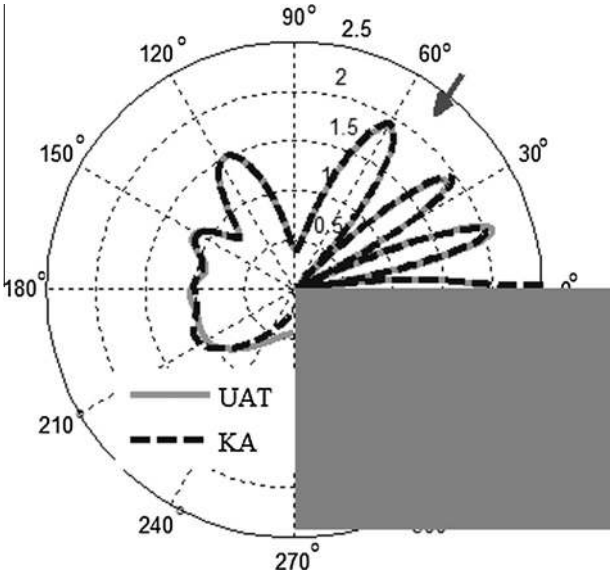

Fig. 9. Comparison between radiation patterns predicted by UAT and KA for a rigid wedge (gray area). $\Phi = 270^\circ$, $\theta_0 = 60^\circ$, $r = 2\lambda$, $\omega = 2\pi^*$ 1 MHz and $c = 2472$ m/s. The amplitude of the total field normalized by the incident one is plotted versus the observation angle θ in a polar diagram.

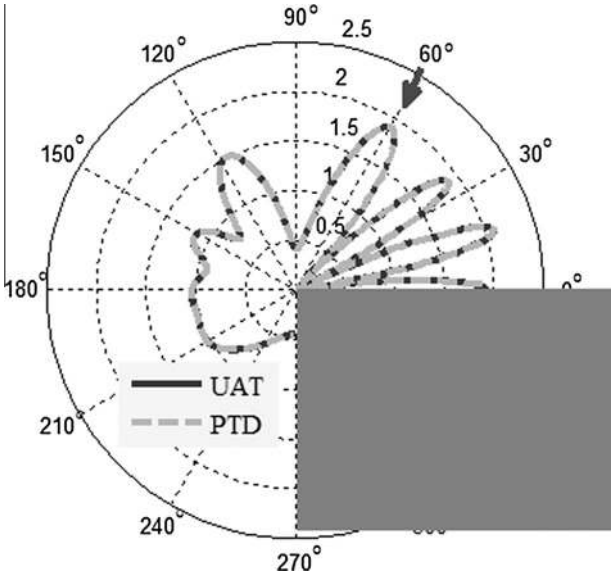

Fig. 10. Comparison between radiation patterns predicted by UAT and PTD for a rigid wedge (gray area). $\Phi = 270°$, $\theta_0 = 60°$, $r = 2\lambda$, $\omega = 2\pi^*$ 1 MHz and $c = 2472$ m/s. The amplitude of the total field normalized by the incident one is plotted versus the observation angle θ in a polar diagram.

Fig. 10 supports the claim that whatever the scattering angle, the scattered PTD field is identical to UAT.

Thus while modeling scatter by a half-plane KA is a very powerful approximation, the KA error can be significant near – and particularly on – the half-plane faces, exhibiting symmetry with respect to the latter. For any other wedge, when only one face is irradiated the error in the shadow exceeds the error in the irradiated region. When both faces are irradiated, the error is more or less the same everywhere except near the surface. When this discrepancy is of importance it can be eliminated by employing PTD.

UAT, UTD and PTD have all proven to be efficient methods for simulating the scattering by the wedge with planar faces. Keeping in mind that telemetry would need to model structures of complex geometry, UAT is the most difficult method to implement, since it involves fictitious reflected rays [16]. UTD requires ray tracing, which accounts for both reflection and diffraction and is the less time consuming method for large targets. PTD is easy to implement using the Kirchhoff integration over the insonified surface and a correction to the edge diffraction field. Finally, unlike UAT and UTD, PTD remains valid at caustics in the fields reflected by curved surfaces [16]. Therefore PTD is the most appropriate tool for simulating ultrasonic telemetry of immersed rigid structures.

4. Conclusion

Several well-known high-frequency approximations have been compared by simulating acoustic scattering by an immersed rigid wedge. It has been confirmed that for a planar wedge UAT, UTD and PTD produce predictions that are the same. Taking into account that PTD requires integration only over the illuminated part of the scattering surface and thus can be easily applied to modeling smooth structures of complex geometry, it is concluded that it is PTD that is most suitable for inclusion in a software tool for simulating the ultrasonic telemetry imaging of immersed rigid structures.

Acknowledgment

Special thanks are due to Dr. Alain Lhémery for his help at the beginning of Bo Lu's thesis, particularly in the part of the project published in [4].

References

[1] F. Reverdy, F. Baqué, B. Lu, K. Jezzine, V. Dorval, J.M. Augem, Simulation of ultrasonic inspection for sodium cooled reactors using CIVA, in: Proceeding of ANIMMA Conf. Ghent, Belgium, 6–9 June, 2011.
[2] F. Jadot, F. Baqué, J.P. Jeannot, J.M. Augem, J. Sibilo, ASTRID sodium cooled prototype: program for improving in service inspection and repair, in: Proceeding of ANIMMA Conf., Ghent, Belgium, 6–9 June, 2011.
[3] M. Darmon, N. Leymarie, S. Chatillon, S. Mahaut, Modelling of scattering of ultrasounds by flaws for NDT, in: Ultrasonic Wave Propagation in Non homogeneous Media, Proc Phys Springer, Springer, vol. 128, 2009, pp. 61 (Chapter 128).
[4] B. Lu, M. Darmon, C. Potel, Stochastic simulation of the high-frequency wave propagation in a random medium, J. Appl. Phys. 112 (5) (2012).
[5] S. Mahaut, M. Darmon, S. Chatillon, F. Jenson, P. Calmon, Recent advances and current trends of ultrasonic modelling in CIVA, Insight 51 (2) (2009) 78–84.
[6] Y.A. Kravtsov, Y.I. Orlov, Geometrical Optics of Inhomogeneous Media, Springer-Verlag, Heidelberg, 1990.
[7] J.B. Keller, Geometrical theory of diffraction, J. Opt. Soc. Am. 52 (1962) 116–130.
[8] R.G. Kouyoumjian, P.H. Pathak, A uniform geometrical theory of diffraction for an edge in a perfectly conducting surface, IEEE Trans. Antennas Propag. 62 (1974) 1448–1461.
[9] S.W. Lee, G.A. Deschamps, A uniform asymptotic theory of electromagnetic diffraction by a curved wedge, IEEE Trans. Antennas Propag. 24 (1) (1976) 25–34.
[10] P.Y. Ufimtsev, Fundamentals of the Physical Theory of Diffraction, John Wiley & Sons, Hoboken, USA, 2007.
[11] M. Born, E. Wolf, A.B. Bhatia, Principles of Optics: Electromagnetic Theory of Propagation, Interference and Diffraction of Light, seventh (expanded) ed., Cambridge U. Press, UK, 1999.
[12] V.M. Babich, M.A. Lyalinov, V.E. Grikurov, Diffraction theory: the Sommerfeld–Malyuzhinets technique, Alpha Science, Oxford, 2008.
[13] V.A. Borovikov, B.Y. Kinber, Geometrical Theory of Diffraction, The Institution of Electrical Engineers, London, United Kingdom, 1994.
[14] B. Lu, M. Darmon, C. Potel, V. Zernov, Models comparison for the scattering of an acoustic wave on immersed targets, J. Phys.: Conf. Ser. 353 (2012) 012009.
[15] Y. Rahmat-Samii, R. Mittra, Spectral analysis of high-frequency diffraction of an arbitrary incident field by a half place – comparison with four asymptotic techniques, Radio Sci. 13 (1) (1978) 31–48.
[16] D. Bouche, F. Molinet, R. Mittra, Asymptotic methods in electromagnetics, Springer, 1997.
[17] F. Molinet, Acoustic High-Frequency Diffraction Theory, Momentum Press, 2011.
[18] V. Zernov, L. Fradkin, M. Darmon, A refinement of the Kirchhoff approximation to the scattered elastic fields, Ultrasonics 52 (7) (2012) 830–835.